

A HUMAN BODY MODEL EXPOSED TO A CLUSTER OF WAVES: A STATISTICAL STUDY OF SAR

O. Jawad^{1, *}, D. Lautru², A. Benlarbi-Delai², J. M. Dricot¹, F. Horlin¹, and P. De Doncker¹

¹OPERA Department, Université Libre de Bruxelles (ULB), 50, Avenue F.D. Roosevelt, Bruxelles 1050, Belgium

²UPMC University Paris 06, UR2, L2E F-75005, Paris, France

Abstract—The impact of wireless channel modeling on exposure to electromagnetic radiation is studied. Two methods are developed in order to assess the statistical properties of whole body Specific Absorption Rate for exposure estimation in indoor environment. The body model is exposed to a bundle of waves, named cluster, following the wireless channel modeling approach. The first method is analytical and based on the Uncorrelated Scattering Assumption of the incident waves. The second method is a classical stochastic method. The point is to identify the parameters of Wireless Channel which led to significant SAR's variation.

1. INTRODUCTION

The study of whole-body exposure to electromagnetic fields emitted by mobile terminals and base stations led to the development of standards and guidelines proposed by the International Commission on Non-Ionizing Radiation Protection (ICNIRP) [1, 2]. Nowadays, numerical dosimetry took an important place into assessing compliance with these guidelines. The evaluation of the exposure is possible by calculating the basic restrictions, the whole body Specific Absorption Rate, SAR_{WB} , in the frequency range 100 kHz–10 GHz:

$$SAR_{WB} = \frac{1}{m} \int_V \frac{\sigma |E|^2}{2} dV \quad (1)$$

with m the human body mass, σ the conductivity of the tissue, $|E|$ the total electric field strength inside the body and V the volume of the body.

Received 8 March 2012, Accepted 15 May 2012, Scheduled 30 May 2012

* Corresponding author: Ourouk Jawad (ojawad@ulb.ac.be).

SAR_{WB} depends on the exposure conditions. A deeper understanding of the electromagnetic environment emerged in the last decade in parallel with the emergence of high performance wireless systems. This knowledge enables to finely simulate the wireless channel parameters which define the exposure conditions.

Most of the numerical dosimetry studies [3–8] do not take into account the wireless channel modeling, especially the cluster concept, in order to assess exposure level. The aim of this paper is to fill in this gap.

In the first part of this paper the wireless channel model in indoor environment will be presented. An analytical study will be developed in order to evaluate the SAR_{WB} . The analytical method will be presented and tested on a cylindrical body model in order to evaluate quickly on a simple body model how many realizations are necessary to reach the convergence with analytical results using a statistical method. The parameters of the wireless channel which lead to significant variation of SAR_{WB} will be highlighted. Comparison with a statistical approach will close the paper. It is worth noting that the aim of this paper is not to reach accurate SAR_{WB} estimations, but to highlight the channel model impact on SAR_{WB} assessment.

2. THE WIRELESS CHANNEL MODEL IN INDOOR ENVIRONMENT

In [9], a Multi-Input Multi-Output (MIMO) indoor channel model is described. It is based on experimental data and identification algorithms. The algorithm of identification detects one by one the channel MultiPath Components (MPCs); the measurements are then statistically analyzed in order to define a stochastic channel model. This model, as the other state-of-the-art channel models, is based on the cluster concept: it has been proven that MPCs propagate as bundles named clusters. Inside each cluster, the MPCs are grouped together in the angular and delay domains (see Figure 1).

Only azimuthal angle is taken into account in our model. All waves are supposed to arrive in an azimuthal propagation plane as we can see in Figure 1, which is a good first approximation in indoor environment [9].

The total electric field can be developed in terms of the MPCs:

$$E_{tot} = \sum_{c=1}^{N_c} \sum_{l=1}^{N_{MPCs}} E_{c,l}(\alpha_{c,l}, \theta_{c,l}, \varphi_{c,l}) \quad (2)$$

with N_c the number of clusters, N_{MPCs} the number of MPCs in each cluster and, respectively, $E_{c,l}$ the electric field, $\alpha_{c,l}$ the amplitude, $\theta_{c,l}$

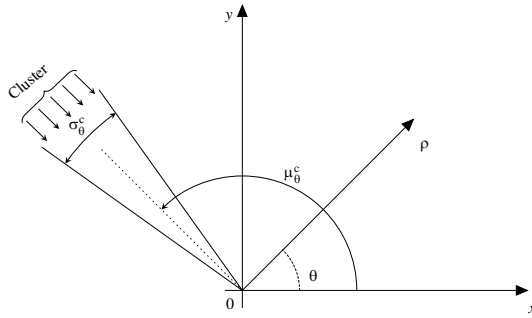


Figure 1. A cluster arriving at the origin of (x, y) axis system.

the angle of incidence and $\varphi_{c,l}$ the phase of l -th MPC of c -th cluster. According to [10], two models can be used in order to define the amplitudes of the MPCs. In the first model, the amplitude follows a standard complex normal probability distribution.

$$\alpha_{c,l} \sim \sqrt{\frac{P_{cl}^c}{2N_{MPCs}}} (\mathcal{N}(0, 1) + j\mathcal{N}(0, 1)) \quad (3)$$

with $\mathcal{N}(0, 1)$ a standard normal probability distribution and P_{cl}^c the power of the cluster. The second model denoted by $\alpha'_{c,l}$, is

$$\alpha'_{c,l} = \sqrt{\frac{P_{cl}^c}{N_{MPCs}}} e^{j\varphi_{c,l}} \quad (4)$$

In that second model, the random phase follows a uniform probability law.

$$\varphi_{c,l} \sim \mathcal{U}(0, 2\pi) \quad (5)$$

In both models, the Uncorrelated Scattering assumption is made, based on the fact that the MPCs arriving from different directions are supposed to be uncorrelated:

$$\langle \alpha_{c,l} \alpha_{c',l'} \rangle = \frac{P_{cl}^c}{N_{MPCs}} \delta_{c,c'} \delta_{l,l'} \quad (6)$$

with $\langle \bullet \rangle$ the expectation of the random variable. The angles of incidence of MPCs are defined thanks to the angular spread and the angle of incidence of the cluster. The angles of incidence of MPCs, $\theta_{c,l}$, follows a normal distribution

$$\theta_{c,l} \sim \mathcal{N}(\mu_{\theta}^c, \sigma_{\theta}^c) \quad (7)$$

with μ_{θ}^c the angle of incidence of the cluster and σ_{θ}^c the angular spread of the cluster. The definition of a cluster requires that the number of

MPCs must be significant otherwise the cluster has no sense (typically 20 MPCs in each cluster). The parameters must verify the following relations:

$$\mu_{\theta}^c = \frac{\sum_{l=1}^{N_{MPCs}} |\alpha_{c,l}|^2 \theta_{c,l}}{P_{cl}^c} \quad (8)$$

$$\sigma_{\theta}^c = \sqrt{\frac{\sum_{l=1}^{N_{MPCs}} |\alpha_{c,l}|^2 (\theta_{c,l} - \mu_{\theta})^2}{P_{cl}^c}} \quad (9)$$

3. ANALYTICAL STUDY

The conditions of exposure are defined from the cluster model, which is stochastic. In that situation, the analysis of the exposure of a body must be done in a statistical sense. In the following development, all the clusters are made of the same number of MPCs, with random complex amplitude. The total field absorbed by the body can be split into its random part and its deterministic part:

$$E_{tot} = \sum_{c=1}^{N_c} \sum_{l=1}^{N_{MPCs}} \mathcal{E}_l(\rho, \theta, \theta_{c,l}) \alpha_{c,l} \quad (10)$$

\mathcal{E}_l represents the normalized electric field (deterministic part) due to the l -th MPC, ρ and θ are the cylindrical coordinates. In order to evaluate the mean of SAR_{WB} and his standard deviation:

$$|E_{tot}|^2 = \sum_{c,d}^{N_c} \sum_{l,m}^{N_{MPCs}} \mathcal{E}_l(\rho, \theta, \theta_{c,l}) \mathcal{E}_m^*(\rho, \theta, \theta_{d,m}) \alpha_{c,l} \alpha_{d,m}^* \quad (11)$$

$$\langle |E_{tot}|^2 \rangle = \sum_{c,d}^{N_c} \sum_{l,m}^{N_{MPCs}} \mathcal{E}_l(\rho, \theta, \theta_{c,l}) \mathcal{E}_m^*(\rho, \theta, \theta_{d,m}) \langle \alpha_{c,l} \alpha_{d,m}^* \rangle \quad (12)$$

Under US assumption:

$$\langle |E_{tot}|^2 \rangle = \sum_{c=1}^{N_c} \sum_{l=1}^{N_{MPCs}} |\mathcal{E}_l(\rho, \theta, \theta_{c,l})|^2 \frac{P_{cl}^c}{N_{MPCs}} \quad (13)$$

So, the mean value of whole body SAR is given by

$$\langle SAR_{WB} \rangle = \frac{1}{m} \sum_{c=1}^{N_c} \frac{P_{cl}^c}{2N_{MPCs}} \sum_{l=1}^{N_{MPCs}} \int_V \sigma |\mathcal{E}_l(\rho, \theta, \theta_{c,l})|^2 dV \quad (14)$$

Its variance is given by

$$\sigma_{SAR_{WB}}^2 = \langle SAR_{WB}^2 \rangle - \langle SAR_{WB} \rangle^2 \quad (15)$$

It is necessary to determine $\langle SAR_{WB}^2 \rangle$, hence $\langle |E_{tot}|^4 \rangle$:

$$\begin{aligned} \langle |E_{tot}|^4 \rangle = & \sum_{c,d,e,f}^{N_c} \sum_{l,m,n,p}^{N_{MPCs}} \mathcal{E}_l(\rho, \theta, \theta_{c,l}) \mathcal{E}_m^*(\rho, \theta, \theta_{d,m}) \mathcal{E}_n(\rho, \theta, \theta_{e,n}) \\ & \mathcal{E}_p^*(\rho, \theta, \theta_{f,p}) \langle \alpha_{c,l} \alpha_{d,m}^* \alpha_{e,n} \alpha_{f,p}^* \rangle \end{aligned} \quad (16)$$

Under US assumption, $\langle |E_{tot}|^4 \rangle - \langle |E_{tot}|^2 \rangle^2$ becomes

$$\langle |E_{tot}|^4 \rangle - \langle |E_{tot}|^2 \rangle^2 = \sum_{c,d}^{N_c} \sum_{l \neq n}^{N_{MPCs}} |\mathcal{E}_l(\rho, \theta, \theta_{c,l})|^2 |\mathcal{E}_n(\rho, \theta, \theta_{c,n})|^2 \left(\frac{P_{cl}^c}{N_{MPCs}} \right)^2 \quad (17)$$

So that

$$\sigma_{SAR_{WB}} = \frac{\sigma}{2m} \sum_{c,d}^{N_c} \frac{P_{cl}^c}{N_{MPCs}} \left[\int_V \sum_{l \neq n}^{N_{MPCs}} |\mathcal{E}_l(\rho, \theta, \theta_{c,l})|^2 |\mathcal{E}_n(\rho, \theta, \theta_{d,n})|^2 dV \right]^{\frac{1}{2}} \quad (18)$$

It is worth noting that results (14) and (18) do not depend on the chosen model for the amplitudes $\alpha_{c,l}$.

4. CYLINDRICAL BODY MODEL

In order to study the impact of the cluster concept on the SAR a simple body model has been chosen. It is made of three homogeneous cylinders which play the role of a trunk and two arms. This model is far away from the accurate existing models used in [11, 12]. The point is not to compare SAR_{WB} with the standards but to estimate the number of realizations that are necessary in order to reach convergence with (14) and (18). The advantage of taking a simple model is twofold. First, this model allows to obtain quick results and to make a lot of realizations with different values of amplitudes. The results obtained from the realizations enable to estimate the number of realizations that are necessary to reach convergence. Secondly, the comparison between analytical and statistical results will ensure the validity of the analytical method and will be usable on accurate body models. This cylindrical body model is represented in Figure 2 in two dimensions and seen from the top. The cylindrical body model is exposed to a TM^z electric field incident from x axis. The complex electric relative permittivity is defined by

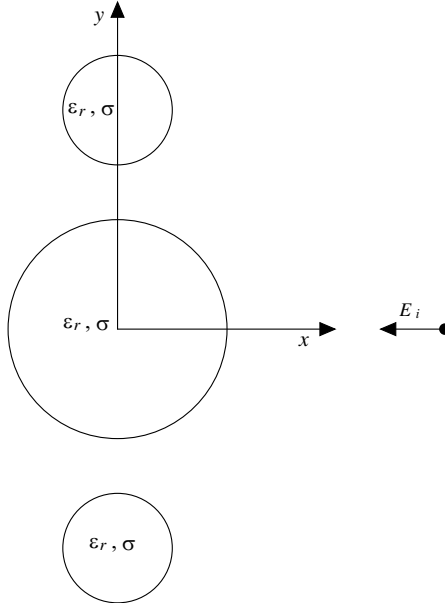


Figure 2. Cylindrical body model exposed to an incident electric field.

$$\tilde{\epsilon}_r = \epsilon_r - j \frac{\sigma}{\epsilon_0 \omega} \quad (19)$$

with ϵ_0 the free space permittivity and ω the angular frequency. The physical and electrical properties of the cylindrical body model are presented in Table 1 [13]. The study was done at frequency $f = 2.45$ GHz. In the case of only one cylinder exposed to a single electromagnetic plane wave, this incident field emitted by a line source in cylindrical coordinates, according to [14], is

$$E_i = \alpha_i \sum_{n=-\infty}^{+\infty} j^{-n} J_n(\beta_0 \rho) e^{jn(\theta - \theta_i)} \quad (20)$$

where the line source is far away from the observation point $\rho_s > \rho$. J_n is the first kind Bessel function, $\beta_0 = \frac{2\pi}{\lambda_0}$ is the number of wave in the free space and θ_i is the angle of incidence of the electromagnetic wave. The arrival of the plane wave at the cylinder will lead to apparition of a scattered field inside and outside the cylinder as a lossless dielectric

Table 1. Physical and electrical properties.

Trunk length (m)	1.80
Trunk radius (m)	0.15
Arms length (m)	0.80
Arms radius (cm)	3.6
Distance arm-trunk (cm)	6.0
Density (kg/m ³)	523.4
Relative permittivity	38.57
Conductivity (S/m)	1.27
Relative Permeability	1

media. The scattered field has the following expression

$$E_s = \begin{cases} \alpha_i \sum_{n=-\infty}^{+\infty} a_n H_n^{(2)}(\beta_0 \rho) e^{jn(\theta-\theta_i)} & \rho > a \\ \alpha_i \sum_{n=-\infty}^{+\infty} b_n J_n(\beta_1 \rho) e^{jn(\theta-\theta_i)} & \rho \leq a \end{cases} \quad (21)$$

with a_n and b_n constant coefficients which depends of the boundary conditions, $H_n^{(2)}$ is the second kind Hankel function, a is the radius of the cylinder and β_1 the number of wave in the cylinder.

$$a_n = j^{-n} \frac{J'_n(\beta_0 a) J_n(\beta_1 a) - \sqrt{\epsilon_r/\mu_r} J_n(\beta_0 a) J'_n(\beta_1 a)}{\sqrt{\epsilon_r/\mu_r} J'_n(\beta_1 a) H_n^{(2)}(\beta_0 a) - J_n(\beta_1 a) H_n^{(2)'}(\beta_0 a)} \quad (22)$$

$$b_n = j^{-n} \frac{J_n(\beta_0 a) H_n^{(2)'}(\beta_0 a) - J'_n(\beta_0 a) H_n^{(2)}(\beta_0 a)}{J_n(\beta_1 a) H_n^{(2)'}(\beta_0 a) - \sqrt{\epsilon_r/\mu_r} J'_n(\beta_1 a) H_n^{(2)}(\beta_0 a)} \quad (23)$$

The electric field inside the body model was computed by using an iterative method described in [15]. Scattered field inside and outside each cylinder are computed at each iteration in order to calculate the total field. For electromagnetic plane wave, ten iterations are computed to calculate the total field.

5. RESULTS

5.1. Scenarios

In order to analyse the impact of the wireless channel parameters on the SAR_{WB} two different cases are considered. They are described in Table 2. In both cases, the body model is exposed to a cluster, its power is set to one watt.

Table 2. Different configurations for studying channel parameters impact.

	Case 1	Case 2
$\alpha_{c,l}$	random	random
μ_θ	fixed to 0°	from 0° to 90°
σ_θ	from 5° to 40°	fixed to 5°
$\theta_{c,l}$	fixed	fixed

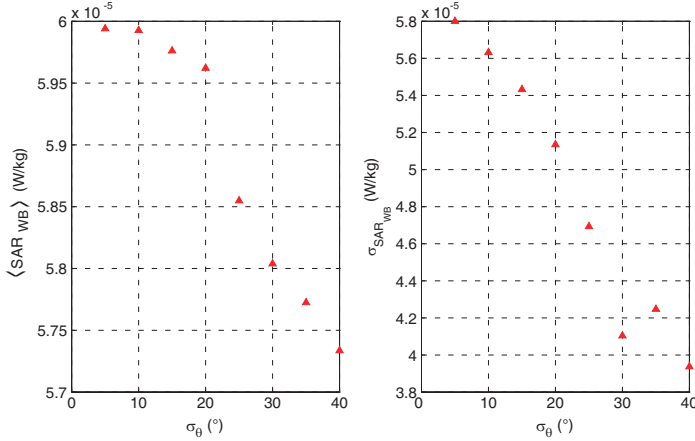


Figure 3. $\langle SAR_{WB} \rangle$ and his standard deviation as a function of the cluster angular spread.

5.1.1. Case 1

As seen in Figure 3, the mean SAR_{WB} and its standard deviation are found to be decreasing while the angular spread increases. The fact that the level of exposure is high when the angular spread is small is due to constructive interference of the MPCs on average in that case. The order of magnitude of standard deviation and mean are the same, meaning that the stochastic nature of exposition cannot be neglected.

5.1.2. Case 2

It can be observed in Figure 4 that the $\langle SAR_{WB} \rangle$ and his standard deviation increases when the angle of incidence increases for an angular spread fixed to 5° . The worst case of exposure is at 90° because the entire cluster is absorbed by the arm. We can also notice that the second case lead to significant fluctuation of $\langle SAR_{WB} \rangle$ and its standard deviation.

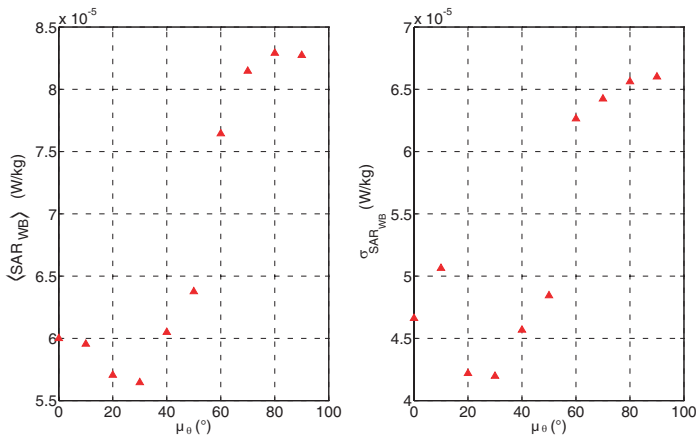


Figure 4. $\langle SAR_{WB} \rangle$ as a function of the cluster angle of incidence.

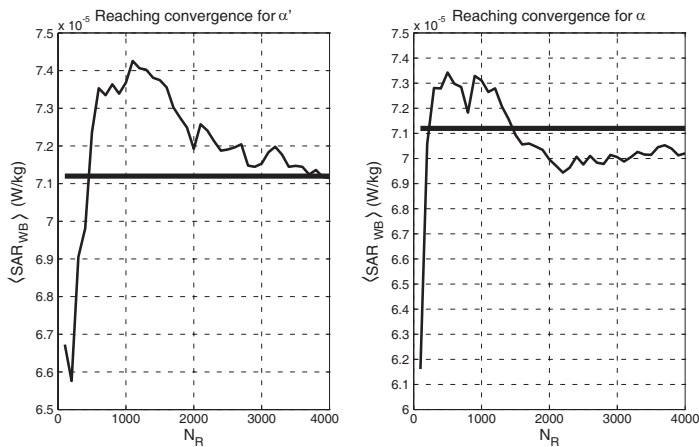


Figure 5. $\langle SAR_{WB} \rangle$ as a function of the number of realizations for both models of amplitude.

5.2. Statistical Study

The aim of the statistical study is to characterize the distribution of SAR_{WB} thanks to a set of N_R realizations. In part 2, it has been shown that the amplitudes can be modelled in two ways, $\alpha'_{c,l}$ or $\alpha_{c,l}$. The comparison between both methods, analytical and statistical, must be done for both models.

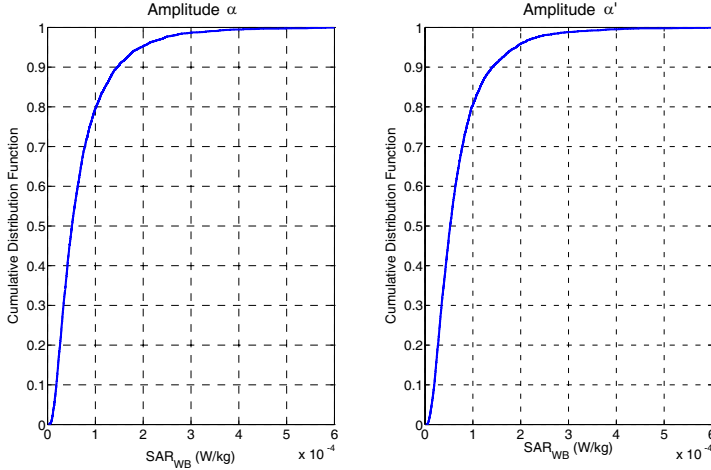


Figure 6. SAR_{WB} CDF for 4000 realizations and for both definitions of amplitude. Note that the Lognormal CDF is not shown because it juxtaposes with SAR_{WB} CDF.

Table 3. Comparison between analytical and statistical methods for $\langle SAR_{WB} \rangle$ and $\sigma_{SAR_{WB}}$ for $N_R = 4000$.

	$\langle SAR_{WB} \rangle$ ($\mu\text{W}/\text{kg}$)	$\sigma_{SAR_{WB}}$ ($\mu\text{W}/\text{kg}$)
Analytical method	71.2	67.0
Statistical method with α'	71.3	67.4
Statistical method with α	70.2	62.7

5.2.1. Comparison between Analytical and Statistical Method

In order to evaluate the number of realizations that are necessary to reach convergence, the cylindrical body model were exposed to one cluster containing twenty MPCs with $(\mu_\theta = 50^\circ, \sigma_\theta = 10^\circ)$.

In Figure 5, the horizontal lines represents the level of the exact value of $\langle SAR_{WB} \rangle$, i.e., the analytical value (14). We can see that the case with amplitude α' reaches the convergence faster than the case with amplitude α .

For α' , the results in Table 4 with $N_R = 4000$ show that there are a relative error between Statistical and Analytical methods of 0.1% for Averaged SAR and 0.6% for standard deviation. For α , the results above show that there are a relative error between Statistical and Analytical methods of 1.4% for Averaged SAR and 6.4% for standard

Table 4. Normal distribution parameters that lead to the Lognormal distributions.

	Analytical values	α	α'
μ [dB]	-9.867	-9.874	-9.866
σ [dB]	0.796	0.802	0.783

deviation. The fact that the relatives errors are higher for the case with amplitude α can be explained by the complexity of α in comparison with α' leading to slower convergence.

5.2.2. Akaike Criterion

The statistical method with $N_R = 4000$ allows to make an analysis of the distribution of SAR_{WB} . The Akaike Criterion [16] was used in order to evaluate the probability that this CDF is the best among the ones that were compared. The criterion select models that best match with the samples by minimizing number of parameters. We compared Normal, Lognormal, Rayleigh, Weibull, Exponential, Poisson, Laplace, Gamma and Rice distributions. The result for Akaike criterion shows that the distribution that best match with our realizations of SAR_{WB} is the Lognormal distribution for both the α' and α models.

In Table 4, the parameters μ and σ of the Lognormal distributions that best match with the SAR_{WB} CDFs is given together with the analytical values (converting (14) and (18) to the μ and σ for a Lognormal distribution) [17].

6. CONCLUSION

In this paper, firstly, analytical expressions of $\langle SAR_{WB} \rangle$ and its standard deviation has been derived. The assessment of the impact of the cluster concept on the SAR has been studied. Thanks to statistical method, it has been shown that SAR follows a Lognormal distribution. This entire study enable us to fully characterize the statistical behaviour of SAR with the exact values ($\langle SAR_{WB} \rangle$ and $\sigma_{SAR_{WB}}$). The impact of wireless channel parameters has been studied and led to significant variation on $\langle SAR_{WB} \rangle$.

REFERENCES

1. ICNIRP, "Guidelines for limiting exposure to time-varying electric, magnetic and electromagnetic fields (up to 300 GHz),"

- Health Physics*, 1998.
2. ICNIRP, "Statement on the guidelines for limiting exposure to time-varying electric, magnetic, and electromagnetic fields (up to 300 GHz)," *Health Physics*, Vol. 97, No. 3, 257–258, Sep. 2009.
 3. Martinez-Burdalo, M., A. Martin, A. Sanchis, and R. Villar, "FDTD assessment of human exposure to electromagnetic fields from wifi and bluetooth devices in some operating situations," *Bioelectromagnetics*, Vol. 30, 142–151, 2009.
 4. Saidi, F., D. Lautru, A. Gati, M. F. Wong, E. Nicolas, F. Jacquin, J. Wiart, and V. Fouad-Hanna, "An on-site 'SAR' evaluation using interpolation and plane-wave decomposition," *Microwave and Optical Technology Letters*, Vol. 50, No. 6, 1501–1505, Jun. 2008.
 5. Joseph, W., G. Vermeeren, L. Verloock, and L. Martens, "Estimation of whole-body SAR from electromagnetic fields using a personal exposure meters," *Bioelectromagnetics*, Vol. 31, 286–295, 2010.
 6. Faraone, A., G. Bit-Babik, and R. Zaridze, "Assessment of human exposure to realistic radio-frequency sources by means of analytical and computational methodologies," *Antennas and Propagation EUCAP*, 1–8, Nov. 2006.
 7. Dlugosz, T. and H. Trzaska, "One experimental setup in bioelectromagnetics," *The Environmentalist*, Vol. 29, No. 2, 124–129, Jun. 2009.
 8. Dlugosz, T. and H. Trzaska, "Proximity effects in the near-field EMF metrology," *IEEE Transactions on Instrumentation and Measurement*, Vol. 58, No. 3, 626–630, Mar. 2009.
 9. Quitin, F., C. Oestges, F. Horlin, and P. De Doncker, "A polarized clustered channel model for indoor MIMO systems at 3.6 GHz," *IEEE Trans. Vehic. Tech.*, 3685–3693, Oct. 2010.
 10. Quitin, F., "Channel modeling for polarized MIMO systems," Ph.D. Dissertation, Université Libre de Bruxelles, 2011.
 11. Conil, E., A. Hadjem, F. Lacroux, M. F. Wong, and J. Wiart, "Variability analysis of SAR from 20 MHz to 2.4 GHz for different adult and child models using finite-difference time-domain," *Phys. Med. Biol.*, Vol. 53, 1511–1525, Feb. 2008.
 12. Kientega, T., E. Conil, A. Hadjem, E. Richalot, A. Gati, M. F. Wong, O. Picon, and J. Wiart, "A surrogate model to assess the whole body SAR induced by multiple plane waves at 2.4 GHz," *Ann. Telecommun.*, Vol. 66, 419–428, May 2011.
 13. Gabriel, S., R. W. Lau, and C. Gabriel, "The dielectric properties

- of biological tissues: III. Parametric models for the dielectric spectrum of tissues,” *Phys. Med. Biol.*, 2271–2293, 1996.
14. Balanis, C. A., *Advanced Engineering Electromagnetics*, John Wiley & Sons, 1989, ISBN 0-471-62194-3.
 15. Liu, L., S. van Roy, P. de Doncker, and C. Oestges, “Azimuth radiation pattern characterization of omnidirectional antennas near a human body,” *Electromagnetics in Advanced Applications, ICEAA '09, International Conference*, 461–464, Turino, Italia, Sep. 2009.
 16. Akaike, H., “A new look at the statistical model identification,” *IEEE Transactions on Automatic Control*, Vol. 19, No. 6, 716–723, 1974.
 17. Ross, M. S., *Introduction to Probability and Statistics for Engineers and Scientists*, Wiley, Jun. 1987.